RSC Advances

ROYAL SOCIETY OF CHEMISTRY

www.rsc.org/advances

GRAPHICAL ABSTRACT

for

Reduced carbon dots employed for synthesizing metal nanoclusters and nanoparticles

Yan Zhuo, Dan Zhong, Hong Miao, Xiaoming Yang*

College of Pharmaceutical Sciences, Education Ministry Key Laboratory on Luminescence and Real-Time Analysis, Southwest University, Chongqing 400715, China

Tel: 86-23-68251225, Fax: 86-23-68251225, E-mail: ming4444@swu.edu.cn.

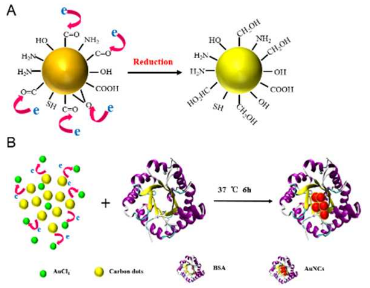

Reduced carbon dots (r-CDs) were creatively and successfully employed for preparing Au nanoclusters and nanoparticles.

RSC Advances RSC**Publishing**

ARTICLE

Reduced carbon dots employed for synthesizing metal nanoclusters and nanoparticles

Cite this: DOI: 10.1039/x0xx00000x

Yan Zhuo, Dan Zhong, Hong Miao, Xiaoming Yang*

Received 00th January 2012,
Accepted 00th January 2012

DOI: 10.1039/x0xx00000x

www.rsc.org/

Carbon dots (CDs) have been considered as ideal and promising fluorescent materials owing to their excellently optical, electronic and biocompatible properties including photoluminescence, photostability, electron transfer behavior and biocompatibility. Interestingly, reduced state carbon dots (r-CDs) emerged as a new type of CDs. Herein, we successfully prepared CDs based on cysteine serving as the carbon source, and further creatively synthesized r-CDs via simply introducing $NaBH_4$ into the solution of CDs. Significantly, this type of r-CDs innovatively played the role of a reducer for directly synthesizing AuNCs and AuNPs (AgNPs), and the reductive groups on their surfaces provided r-CDs with the excellent electron donating capability, thereby facilitating to fast reduce metal ions as corresponding metal nanoclusters or nanoparticles. Besides, this exploration may open a new scope of CDs's applications in synthesis of metal nanomaterials.

Introduction

Carbon dots (CDs), known as small oxygenous carbon nanoparticles (<10 nm), have been emerging as superior fluorescent nanomaterials owing to their excellent properties including low cytotoxicity,[1] biocompatibility,[2] photoluminescence,[3] photostability and electron transfer behavior.[4] Thus, CDs have received significant attentions as a promising alternative to traditional semiconducting quantum dots. Interestingly, enhanced electron transfer is related with the surface passivation of carbon dots, which provides new opportunities for energy conversion and other applications.[5-9] For instance, Yu et al. designed a method of employing CDs as the energy donor for detecting H_2S[10] and CDs also have been used as visible-light photocatalysts to reduce CO_2 more efficiently.[11]

For their structures, most CDs rather than nanodiamonds were composed of sp^2 carbon atoms hybridized with abundant oxygenous residues, and it is proved that there exist oxygen-containing functional groups (hydroxyl groups, carbonyl, carboxyl and epoxy) on their surfaces.[12] Consequently, CDs certainly play roles as both electron acceptors and electron donors,[13] describing their potential as an oxidizing or reducing agent. The electron-donating capability of CDs has been successfully verified by reducing metal salts to its corresponding metal.[14, 15] For example, Shi et al. reported synthesis of Au@CDs by utilizing surface enhanced Raman scattering (SERS);[16] Lv et al. obtained Ag@CDs composite according to the reduction of $Ag(NH_3)_2OH$ by CDs themselves.[17] However, these methods suffered from disadvantages like high synthesis-temperature and introductions of additional chemicals.[18] To date, however, studies on synthesizing noble-metal nanomaterials by using CDs as reducing agents have not been addressed.

Basically, preparations of CDs are mainly achieved by treating various carbon sources such as graphite,[19-21] soot from a burning candle[22, 23] and natural gas,[24] saccharide[25] and graphene oxide (GO)[1, 26] through oxidation processes. As a result, most CDs appear in high oxidation forms and this oxidation does not facilitate the fluorescence emission of CDs, but reduction of CDs display enhanced fluorescence.[27,28] Thus, developing reduced CDs will broaden their meaningful applications.

Noble metal nanoclusters (NCs), typically consisting of several to tens of atoms, have attracted numerous researchers during recent years due to their unique physical, electrical, and optical properties.[29] Among metal NCs, AuNCs have been extensively studied because oftheir intrinsic characteristics like facile synthesis, chemical stability, and high quantum yield.[30-32] So far, a few reducers mainly referring to sodium bornhydride ($NaBH_4$),[33, 34] sodium citrate[35, 36] and ascorbic acid (Vc)[37] have been introduced to synthesize AuNCs.

For the conventional methods of synthesizing Au or Ag nanoparticles (AuNPs or AgNPs), sodium citrate or $NaBH_4$

usually serves as reducing agents.[32] In addition, alcohols sometimes acted as reducing agent for synthesis of metal nanoparticles.[38, 39]As previously reported, the oxyethylene groups on the surface of poly (ethylene glycols) showed reducing ability for reducing Au $^{3+}$or Ag^{+} to form gold or silver nanoparticles.[40,41] Also, poly (vinyl pyrrolidone) terminating with the hydroxyl group (–OH) was employed to prepare nanoparticles, proving the reducing function of –OH.[42, 43]

Herein, we first creatively prepared carbon dots based on cysteine serving as the carbon source, and further successfully synthesized r-CDs via simply adding $NaBH_4$ into the solution of CDs. Importantly, this type of r-CDs were first successfully employed for preparing Au nanoclusters and nanoparticles. This exploration may open a new field of applications of CDs, especially for synthesis of metal nanomaterials.

Experimental

Apparatus

All fluorescence measurements were performed on a Hitachi F-7000 fluorescence spectrophotometer (Tokyo, Japan) with excitation slit set at 5 nm band pass and emission at 5 nm band pass in 1 cm × 1 cm quartz cell. Meanwhile, UV/vis absorption spectra were recorded by a Shimadzu UV-2450 spectrophotometer (Tokyo, Japan). High-resolution transmission electron microscopy (HR-TEM) images were obtained by using a TECNAI G^2 F20 microscope (FEI, America) at 200 KV. Samples for HR-TEM analysis were prepared by evaporating a drop of aqueous product on a lacey carbon copper TEM grid. Fourier transform infrared (FTIR) spectra were recorded on a Thermo Nicolet-380 IR spectrophotometer with the KBr pellet technique ranging from 400 to 4000 cm^{-1} (Tokyo, Japan). X-ray photoelectron spectroscopy (XPS) analysis was performed on a PHI 5000 Versaprobe system, using monochromatic Al Kα radiation (1486.6 eV) operating at 25 W (Shimadzu, Japan). The quantum yields were obtained by an Absolute PL quantum yield spectrometer C11347 (Hamamatsu, Japan). The powder of CDs, r-CDs and r-CDs-AuNCs were obtained by lyophilisation in PiloFD8-4.3V (Charlotte, USA). Mass spectra were obtained by UltrafleXtreme Matrix-assisted laser desorption/ionization-time-of-flight mass spectrometry (MALDI TOF/TOF MS, USA). A Fangzhong pHS-3C digital pH meter (Chengdu, China) was employed to measure the pH values of various aqueous solutions and a vortex mixer QL-901 (Haimen, China) was used for blending the solution. Zeta potential was measured after suitably diluting CDs and r-CDs solutions at 25.0 ± 0.5℃, using a Nano Zetasizer (Malvern, England). The thermostatic water bath (DF-101s) was purchased from Gongyi Instrument Co., Ltd (Gongyi, China).

Chemicals and materials

Chloroauric acid ($HAuCl_4$, M_w=411.85, AR), albumin from bovine serum (BSA) and silver nitrate ($AgNO_3$, M_w=169.87, AR) and cysteine (cys) were obtained from Shanghai Sangon Biotechnology Co., Ltd (Shanghai, China). Sodium hydroxide (NaOH, M_w=40.00, AR), sodium citrate, ascorbic acid (Vc, M_w=176.12, AR), sodium borohydride ($NaBH_4$, M_w=37.83, AR) and hydrazine hydrate (80%) were purchased from Dingguo Changsheng Biotechnology Co., Ltd (Beijing, China). Ultrapure water, 18.25 MΩ • cm, produced with an Aquapro AWL-0502-P ultrapure water system (Chongqing, China) was employed for all the experiments.

Synthesis of CDs and r-CDs

Cysteine (1.5g) was initially added to ultrapure water (2mL) and mixed with NaOH (2M, 1mL). Then, this mixture was heated in a domestic 750W microwave oven for 3 min. Meanwhile, the solution varied from a colorless liquid to a yellowish and finally clustered solid. After cooled to room temperature, this solid was dissolved with 10 mL ultrapure water. An aqueous solution of the CDs was purified by centrifuging (3000 rpm, 15min) to remove large or agglomerated particles. Finally, the fluorescent carbon dots were collected by dialysis against deionized water via a dialysis membrane (300MWCO) for 24 h. The powder of CDs was obtained by lyophilisation, and further dissolved in ultrapure water with a final concentration of mg·mL^{-1}. The purified CDs prepared here were kept at 4 ℃ prior to use.

Next, sodium borohydride (0.05 g) was introduced into the CDs solution (1mg·mL^{-1}, 20mL) obtained above and then stirred gently overnight at room temperature. Excess reducer was removed by dialysis as mentioned above.

Synthesis of r-CDs-AuNCs

In a typical procedure, an aqueous $HAuCl_4$ solution (300 μL, 10 mM) was added into the r-CDs solution (200 μL, 1 mg·mL^{-1}) under vigorous stirring at 37℃. Subsequently, BSA (300 μL, 50mg·L^{-1}) was introduced at 37 ℃, and this mixture was incubated at 37 ℃ for 12 h.

Preparation of r-CDs-AgNPs

The r-CDs-AgNPs were prepared by treating $AgNO_3$ aqueous solution in the presence of r-CDs. As a typical run, 200 μL of r-CDs (1 mg·mL^{-1}) and 150 μL of $AgNO_3$ (10 mM) were mixed and incubated at 50 ℃ in a water bath for 10min, and the color of this solution varied from light yellow to dark brown, suggesting that the reduction of Ag ions to Ag nanoparticles finished. The products were washed three times with ultrapure water by centrifugation at 8000 rpm for 10min.

Preparation of r-CDs-AuNPs

Similarly, 1 mL r-CDs (1 mg·mL^{-1}) solution was mixed with 200 μL, 10 mM of $HAuCl_4$, then this mixture was incubated at 60 ℃ in a water bath for 30 min, and the color of this solution varied from light yellow to wine-red, indicating that the reduction of Au ions to Au nanoparticles finished. The products were washed three times with ultrapure water by centrifugation at 8000 rpm for 10 min.

Results and discussion

To explore their properties of CDs and r-CDs initially, a series of characterizations were performed. As shown in Fig. 1A, the original CDs exhibited maximum excitation and emission wavelengths at 410 nm and 475 nm, respectively. However, the r-CDs was excited at 370 nm and surface structure facilitated this blue shift of the emission peak for r-CDs. Simultaneously, brighter blue fluorescence of r-CDs appeared compared with that of CDs, and the fluorescence of their related lyophilized powder (Fig. S1, ESI†) showed an agreement with that of Fig. 1A. Besides, the CDs displayed more obvious excitation-dependent behavior than r-CDs, and similar infrared upconversion property for the two types of CDs were observed (Fig. S2, ESI†). The average QYs of the r-CDs were obtained around 31.4%, while that of CDs were about 4.7% (Table S1, ESI†). These data above demonstrated that r-CDs showed superior fluorescent properties than CDs.

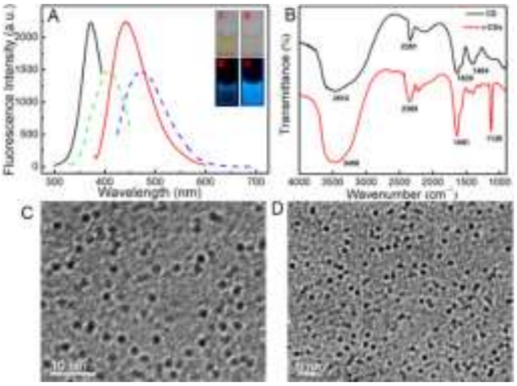

Fig. 1 (A) The maximum excitation and emission spectra of CDs and r-CDs (inset: photographs under visible light (Ⅰ, Ⅲ) and UV light (Ⅱ, Ⅳ) respectively; (B) FTIR of CDs and r-CDs; HR-TEM images of CDs (C) and r-CDs (D).

Next, fourier transform infrared spectroscopy (FTIR) and X-ray photoelectron spectroscopy (XPS) were applied to explore the surface groups, structure and components of CDs and r-CDs in detail. As revealed in Fig. 1B, there were O-H, N-H, C=O, S-H, and C-N, C-O groups on the surface of both CDs and r-CDs. Specifically, the absorption bands of O-H and N-H stretching vibrations appeared at 3510 cm^{-1} and 3496 cm^{-1}. Howbeit, the vibrational absorption band of C=O at 1639 cm^{-1} shifted to 1651 cm^{-1}, indicating that the surface carbonyl groups of the CDs have been reduced.[38] Furthermore, XPS analysis also showed that the carbonyl peak at 287.9 eV obviously decreased after reduction, whereas sp^2 C=C peak at 284.5 eV retained its original intensity (Fig. S3, ESI†). The S_{2p} XPS spectrum demonstrated a peak at 163.9 eV corresponding to the binding energy for the C–S bond, owing to their spin–orbit couplings. And S-H peak at 164.6 eV revealed that there existed S-H in the two types of CDs. The latter peak can be fit with oxidized sulfur species at 167.6 eV originated from a C–SOx (x = 2, 3, 4) species such as sulfate or sulfonate.[45,46] (Fig. S4, ESI†) Moreover, these oxygen-containing surface groups (hydroxyl, carbonyl and carboxyl) resulted in CDs more hydrophilic and negatively charged. The r-CDs zeta potential value were about -20 mV (pH = 7.0) as well as the CDs zeta potential value of about -11.1 mV (pH= 7.0) (Table. S1, ESI†). This above evidence shows that the CDs were reduced by $NaBH_4$ and that $NaBH_4$ selectively reduced the carbonyl to hydroxyl groups and without reducing other species (C=C and COOH). Again, a high resolution transmission electron microscope (HR-TEM) image was employed to directly observe the morphology and particle size distributions. As shown in Fig. 1C and 1D, no aggregation of CDs occurred, depicting their satisfactory dispersion. In particular, the size distribution of CDs was 1-3 nm with the average diameter of 2.0 nm. Meanwhile, r-CDs remained well dispersed after reduction with their related average size of about 2.3 nm (Fig. S5, ESI†).

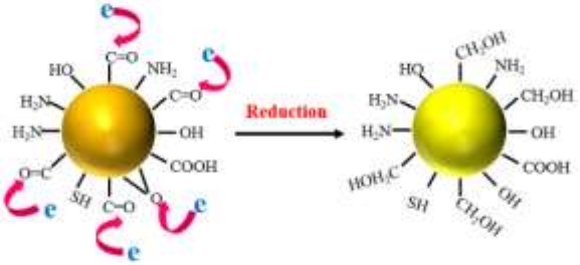

Fig. 2 Schematic illustration of synthesizing reduced-state carbon dots.

To elucidate the formation mechanism of r-CDs, we have built up a model for this reduction process (Fig. 2). To be specific, $NaBH_4$ selectively reduced carbonyl and epoxy rather than other species (C=C and COOH), inducing the increased amount of hydroxyl groups on the r-CDs. Meaningfully, the increased amount of hydroxyl groups endowed the reducibility of r-CDs.[44]

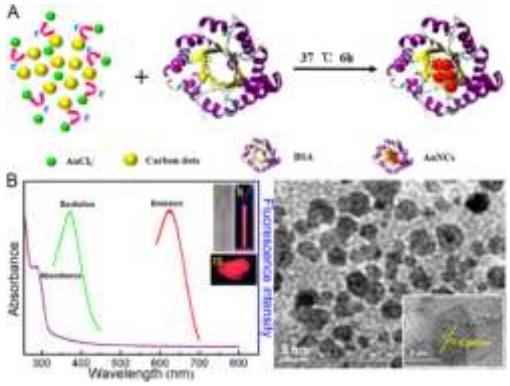

Fig. 3 (A) Schematic illustration of preparing r-CDs-AuNCs; (B) Fluorescence excitation and emission spectra of r-CDs-AuNCs. Inset: photographs of r-CDs-AuNCs solution (I, II) and powder (III); (C) HR-TEM image of r-CDs-AuNCs (Inset: the crystalline structure of an individual nanocluster and the histogram of the size distribution).

Considering the advantage of their reducibility, we addressed that whether r-CDs can be utilized to prepare nanoclusters. Taken r-CDs, $HAuCl_4$ and BSA into account, r-CDs-AuNCs were successfully synthesized on the basis of the electron transfer from r-CDs (Fig. 3A). To describe this AuNCs, the brown solution of r-CDs-AuNCs exhibited the excitation and emission peaks at 375 and 630 nm respectively with its related visualization (photogragh Ⅰ and Ⅱ). At the same time, the powder of r-CDs-AuNCs via lyophilisation exhibited striking red fluorescence under UV light (photogragh Ⅲ), whereas yellowish was observed under daylight. To investigate the nanostructures of r-CDs-AuNCs, HR-TEM was employed to directly observe the morphology and particle size distributions. As shown in Fig. 3C, r-CDs-AuNCs obtained here existed with a major population within the size range of 2-3 nm and no aggregation emerged. Next, FTIR spectroscopy revealed the groups of this AuNCs. In particular, there are the fractions of -NH_2, -OH and C=O upon the formation of the r-CDs-AuNCs (Fig. S6, ESI†). Furthermore, matrix-assisted laser desorption/ionization time-of-flight (MALDI-TOF) mass spectrometry was applied to characterize the current AuNCs. As shown in Fig. S7 (ESI†), the as-prepared r-CDs-AuNCs exhibited a peak at 70 kDa, and BSA molecular weight of 66 kDa was well-known. Thereby, the r-CDs-AuNCs showed a peak shift of ~4 kDa, suggesting that there were 21 gold atoms in r-CDs-AuNCs. In accordance with the FT-IR data, MS results provided further evidence of r-CDs-AuNCs formation.

Likewise, the r-CDs-AuNCs displayed excitation-independent behavior (Fig. S8, ESI†), describing their stable fluorescent property. Additionally, the r-CDs only reduced by $NaBH_4$ showed efficiency for synthesizing r-CDs-AuNCs with distinct fluorescence, indicating that $NaBH_4$ rather than other reducers can be used for reducing CDs towards the synthesis of AuNCs (Fig. S9, ESI†). To identify the optimized conditions of synthesizing r-CDs-AuNCs, a series of experiments were further performed. As revealed in Fig. S10 (ESI†), the fluorescence intensity of r-CDs-AuNCs exhibited variations along with varying concentrations of r-CDs and Au^{3+}, demonstrating that synthesis of r-CDs-AuNCs were dependent on these proposed factors. Thus, 2.0 g·L^{-1} of r-CDs and 3.0 mM of Au^{3+} served as the optimal conditions.

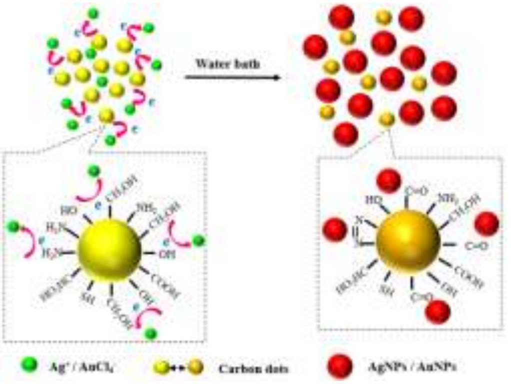

Fig. 4 Schematic illustration of preparing r-CDs-metal nanoparticles.

Since the r-CDs described here behaved as an effective reducer, we further asked whether they can be employed for synthesizing AuNPs or AgNPs. Importantly, we have successfully prepared AgNPs and AuNPs by using r-CDs without any additional reducing agent or external photoirradiation under a mild water-bathing condition (Fig. 4). For the mechanism, r-CDs acted as an electron donor for ensuring the reduction of metal ions to atoms.[47] To be specific, Ag^+ (Au^{3+}) were firstly attracted to the surface of r-CDs via electrostatic interactions with hydroxyl, amine, and other functional groups. Then, Ag^+ (Au^{3+}) ions were reduced by r-CDs via electron transfer from r-CDs to metal ions.[48] Eventually, Ag or Au atoms functioned as the nucleation center and followed by the growth of metallic nanocrystal, leading to formations of AgNPs or AuNPs. During this process, r-CDs also played the role of a stabilizer, preventing AgNPs and AuNPs away from aggreations.[15]

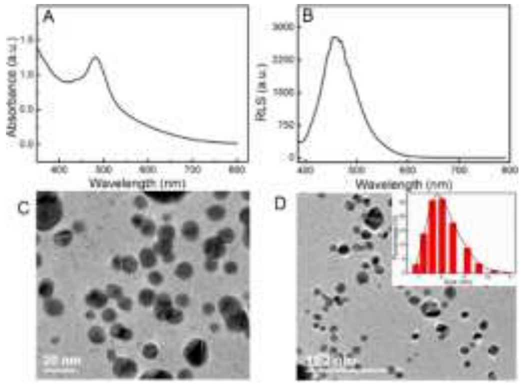

Fig. 5 (A) UV-vis spectra of r-CDs-AgNPs; (B) RLS spectra of r-CDs-AgNPs; (C, D) HR-TEM images of r-CDs-AgNPs. Insert: DLS data of r-CDs-AgNPs.

Next, various characterizations of the AgNPs obtained by using r-CDs were performed. Compared with the original r-CDs, the mixture including r-CDs and AgNPs apparently exhibited the lower fluorescence intensity and a red-shift of about 30 nm as well as the solution color varying from light yellow to brown (Fig. S11, ESI†). As illustrated in UV-vis spectra (Fig. 5A), the adsorption band of r-CDs-AgNPs at 480 nm was attributed to the characteristic surface plasmon absorption of r-CDs-AgNPs, and their related resonance light scattering (RLS) was at 480 nm (Fig. 5B). Taken together, the data above demonstrated that r-CDs-AgNPs indeed formed by virtue of r-CDs. Towards the nanostructure of r-CDs-AgNPs, HR-TEM was employed to directly observe the morphology and particle size distributions. As shown in Fig. 5 C and D, r-CDs-AgNPs obtained here existed as a major population at the size of 8 nm and no aggregation emerged. For the size distribution analysis, the diameter of r-CDs-AgNPs existed in the range of 6-10 nm determined by dynamic light scattering (DLS).

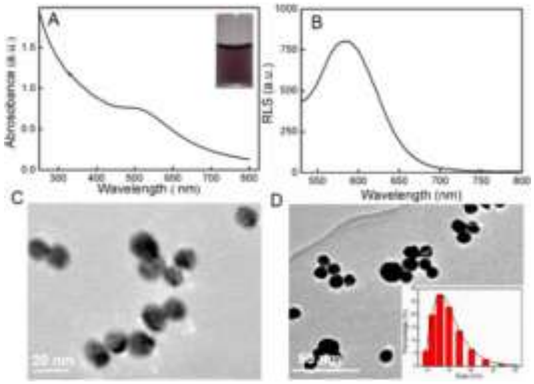

Fig. 6 (A) UV-vis spectra of r-CDs-AuNPs; (B) RLS spectra of r-CDs-AuNPs; (C, D) HR-TEM images of r-CDs-AuNPs. Insert: DLS data of r-CDs-AuNPs.

Again, different kinds of r-CDs reduced by $NaBH_4$, ascorbic acid, citrate sodium, and hydrazine hydrate respectively were introduced to synthesize AgNPs. As shown in Fig. S12 (ESI†), only the solution in the presence of r-CDs derived from $NaBH_4$ showed an absorption band, indicating that other reducers except $NaBH_4$ can't be applied to synthesize r-CDs for further reducing Ag^+ to AgNPs. Furthermore, to identify the appropriate conditions of synthesizing r-CDs-AgNPs, various experiments were performed. As revealed in Fig. S13 (ESI†), the absorbance intensities of r-CDs-AgNPs implied variations along with varying concentrations of r-CDs and Ag^+, reaction time and temperature, demonstrating that synthesis of r-CDs-AgNPs were dependent on these selected conditions. Thereby, 2.0 g·L^{-1} of r-CDs, 2.0 mM of Ag^+, 50 °C and 10 min finally served as the optimal conditions.

Similarly, we also obtained AuNPs by r-CDs. In UV-vis spectra, the adsorption band at 520 nm was attributed to the characteristic surface plasmon absorption of r-CDs-AuNPs, and the obvious RLS was at 570 nm (Fig. 6A and B), describing the formation of AuNPs. TEM images and DLS showed that r-CDs-AuNPs are uniformly distributed, and their size was 13.4 ± 7.3 nm in Fig. 6 C and D. Besides, these data proved that AuNPs formed only in the presence of r-CDs reduced by $NaBH_4$ (Fig. S14, ESI†), indicating the agreement with that of preparing AgNPs. Likewise, we further identified the optimized conditions for synthesizing AuNPs as 1.0 g·L^{-1} of r-CDs, 1.5 mM of Au^{3+}, 60 ℃ and 30 min (Fig. S15, ESI†).

Conclusions

In conclusion, we have successfully synthesized r-CDs by reducing conventional CDs, while cysteine served as the carbon source. Meaningfully, metal nanoclusters and nanoparticles were creatively prepared by using the r-CDs as a reducing agent on the basis of electron transfer. To be specific, the hydroxyl groups on their surfaces provided r-CDs with the excellent electron donating capability, thereby facilitating to fast reduce metal ions as corresponding metal nanoclusters or nanoparticles. Significantly, this electron transfer mechanism of r-CDs will broaden their potential applications in the fields of energy-conversion systems or catalysis such as solar cells, electro-catalysis and photo-catalysis.

Acknowledgements

We gratefully acknowledge financial support by National Natural Science Foundation of China (31100981), Research Fund for the Doctoral Program of Higher Education of China (20110182120014), Natural Science Foundation Project of CQ CSTC (cstc2013jcyjA10117), Fundamental Research Funds for the Central Universities (XDJK2013B038, 2362014xk07), and Program for Innovative Research Team in University of Chongqing (2013).

Notes and references

College of Pharmaceutical Sciences, Education Ministry Key Laboratory on Luminescence and Real-Time Analysis, Southwest University, Chongqing 400715, China. Fax: 862368251225; Tel: 862368251225. E-mail: ming4444@swu.edu.cn.

† Electronic Supplementary Information (ESI) available: [details of any supplementary information available should be included here]. See DOI: 10.1039/b000000x/

1. H. T. Li, X. D. He, Z. H. Kang, H. Huang, Y. Liu, J. L. Liu, S. Y. Lian, C. H. A. Tsang, X. B. Yang and S. T. Lee, *Angew. Chem. Int. Edit.*, 2010, **49**, 4430-4434.
2. S. N. Baker and G. A. Baker, *Angew. Chem. Int. Edit.*, 2010, **49**, 6726-6744.
3. S. T. Yang, L. Cao, P. G. J. Luo, F. S. Lu, X. Wang, H. F. Wang, M. J. Meziani, Y. F. Liu, G. Qi and Y. P. Sun, *J. Am. Chem. Soc.*, 2009, **131**, 11308.
4. F. Wang, Y. H. Chen, C. Y. Liu and D. G. Ma, *Chem. Commu.*, 2011, **47**, 3502-3504.
5. H. T. Li, Z. H. Kang, Y. Liu and S. T. Lee, *J. Mater. Chem.*, 2012, **22**, 24230-24253.
6. S. Y. Park, H. U. Lee, E. S. Park, S. C. Lee, J. W. Lee, S. W. Jeong, C. H. Kim, Y. C. Lee, Y. S. Huh and J. Lee, *Acs Appl. Mater. Inter.*, 2014, **6**, 3365-3370.
7. Q. Xu, P. Pu, J. Zhao, C. Dong, C. Gao, Y. Chen, J. Chen, Y. Liu and H. Zhou, *J. Mater. Chem. A.*, 2015, **3**, 542-546.
8. W. Lu, X. Qin, S. Liu, G. Chang, Y. Zhang, Y. Luo, A. M. Asiri, A. O. Al-Youbi and X. Sun, *Anal. Chem.*, 2012, **84**, 5351-5357.
9. X. T. Zheng, A. Than, A. Ananthanaraya, D.-H. Kim and P. Chen, *ACS nano*, 2013, **7**, 6278-6286.
10. C. M. Yu, X. Z. Li, F. Zeng, F. Y. Zheng and S. Z. Wu, *Chem. Comm.*, 2013, **49**, 403-405.
11. L. Cao, S. Sahu, P. Anilkumar, C. E. Bunker, J. A. Xu, K. A. S. Fernando, P. Wang, E. A. Guliants, K. N. Tackett and Y. P. Sun, *J. Am. Chem. Soc.*, 2011, **133**, 4754-4757.
12. X. C. Wang, Z. Y. Li and M. P. Doyle, *Chem. Comm.*, 2009, 5612-5614.
13. X. Wang, L. Cao, F. S. Lu, M. J. Meziani, H. Li, G. Qi, B. Zhou, B. A. Harruff, F. Kermarrec and Y. P. Sun, *Chem. Comm.*, 2009, 3774-3776.
14. L. M. Shen, M. L. Chen, L. L. Hu, X. W. Chen and J. H. Wang, *Langmuir*, 2013, **29**, 16135-16140.
15. L. M. Shen, Q. Chen, Z. Y. Sun, X. W. Chen and J. H. Wang, *Anal. Chem.*, 2014, **86**, 5002-5008.
16. P. Luo, C. Li and G. Shi, *Phys. Chem. Chem. Phys.*, 2012, **14**, 7360-7366.
17. Q. Wang, H. Song, Y. Hu, Y. Su and Y. Lv, *RSC Advances*, 2014, **4**, 3992.
18. Y. Zhang, C. Xing, D. Jiang and M. Chen, *CrystEngComm*, 2013, **15**, 6305-6310.
19. H. Zhu, X. L. Wang, Y. L. Li, Z. J. Wang, F. Yang and X. R. Yang, *Chem. Ccomm.*, 2009, 5118-5120.
20. L. Y. Zheng, Y. W. Chi, Y. Q. Dong, J. P. Lin and B. B. Wang, *J. Am. Chem. Soc.*, 2009, **131**, 4564.
21. Y. Q. Dong, N. N. Zhou, X. M. Lin, J. P. Lin, Y. W. Chi and G. N. Chen, *Chem. Mater.*, 2010, **22**, 5895-5899.
22. H. P. Liu, T. Ye and C. D. Mao, *Angew. Chem. Int. Edit.*, 2007, **46**, 6473-6475.
23. S. C. Ray, A. Saha, N. R. Jana and R. Sarkar, *J. Phys. Chem. C.*, 2009, **113**, 18546-18551.
24. L. Tian, D. Ghosh, W. Chen, S. Pradhan, X. J. Chang and S. W. Chen, *Chem. Mater.*, 2009, **21**, 2803-2809.
25. H. Peng and J. Travas-Sejdic, *Chem. Mater.*, 2009, **21**, 5563-5565.
26. J. H. Shen, Y. H. Zhu, C. Chen, X. L. Yang and C. Z. Li, *Chem. Comm.*, 2011, **47**, 2580-2582.

27. Y. Xu, M. Wu, X. Z. Feng, X. B. Yin, X. W. He and Y. K. Zhang, *Chem-Eur. J.*, 2013, **19**, 6282-6288.
28. L. Wang, S. J. Zhu, H. Y. Wang, S. N. Qu, Y. L. Zhang, J. H. Zhang, Q. D. Chen, H. L. Xu, W. Han, B. Yang and H. B. Sun, *Acs Nano*, 2014, **8**, 2541-2547.
29. L. Shang, S. J. Dong and G. U. Nienhaus, *Nano Today*, 2011, **6**, 401-418.
30. J. Chen, Q. F. Zhang, T. A. Bonaccorso, P. G. Williard and L. S. Wang, *J. Am. Chem. Soc.*, 2014, **136**, 92-95.
31. R. C. Jin, *Nanoscale*, 2010, **2**, 343-362.
32. Z. K. Wu and R. C. Jin, *Nano Lett.*, 2010, **10**, 2568-2573.
33. Z. K. Wu, M. Wang, J. Yang, X. H. Zheng, W. P. Cai, G. W. Meng, H. F. Qian, H. M. Wang and R. C. Jin, *Small*, 2012, **8**, 2028-2035.
34. X. Yang, M. Shi, R. Zhou, X. Chen and H. Chen, *Nanoscale*, 2011, **3**, 2596.
35. T. A. C. Kennedy, J. L. MacLean and J. W. Liu, *Chem. Comm.*, 2012, **48**, 6845-6847.
36. J. Zheng, J. T. Petty and R. M. Dickson, *J. Am. Chem. Soc.*, 2003, **125**, 7780-7781.
37. Y. P. Bao, C. Zhong, D. M. Vu, J. P. Temirov, R. B. Dyer and J. S. Martinez, *J. Phys. Chem. C.*, 2007, **111**, 12194-12198.
38. J. J. Deng, P. Yu, Y. X. Wang, L. F. Yang and L. Q. Mao, *Adv. Mater.*, 2014, **26**, 6933-6943.
39. B. Tang, J. L. Li, X. L. Hou, T. Afrin, L. Sun and X. G. Wang, *Ind. Eng. Chem. Res.*, 2013, **52**, 4556-4563.
40. B. Wiley, T. Herricks, Y. G. Sun and Y. N. Xia, *Nano Lett.*, 2004, **4**, 2057-2057.
41. Y. Wang, J. W. Ren, K. Deng, L. L. Gui and Y. Q. Tang, *Chem. Mater.*, 2000, **12**, 1622-1627.
42. Y. J. Xiong, I. Washio, J. Y. Chen, H. G. Cai, Z. Y. Li and Y. N. Xia, *Langmuir*, 2006, **22**, 8563-8570.
43. I. Washio, Y. J. Xiong, Y. D. Yin and Y. N. Xia, *Adv. Mater.*, 2006, **18**, 1745.
44. H. Z. Zheng, Q. L. Wang, Y. J. Long, H. J. Zhang, X. X. Huang and R. Zhu, *Chem. Comm.*, 2011, **47**, 10650-10652.
45 Y. L. Li, J. J Wang, X. F Li, D. S. Geng, M. N. Banis, Y. J Tang, D. N. Wang, R. Li, T. K. Sham, X. L, Sun. *J. Mater. Chem.*, 2012, **22**, 20170–20174.
46 S. Yang, L.J Zhi, K. Tang, X.L. Feng, J. Maier, K. Müllen. *Adv. Funct. Mater.* 2012, **22**, 3634–3640.
47. Y. Choi, G. H. Ryu, S. H. Min, B. R. Lee, M. H. Song, Z. Lee and B.-S. Kim, *ACS nano*, 2014.
48. H. Choi, S. J. Ko, Y. Choi, P. Joo, T. Kim, B. R. Lee, J. W. Jung, H. J. Choi, M. Cha, J. R. Jeong, I. W. Hwang, M. H. Song, B. S. Kim and J. Y. Kim, *Nat Photonics*, 2013, **7**, 732-738.